An orange-light-emitting cationic iridium(III) complex containing a carbazole-oxadiazole bipolar unit: synthesis and application for $Y_3Al_5O_{12}:Ce^{3+}$-based neutral/warm white LEDs

M. F. ZHANG[1], Y. C. YE[2], Y. Q. WEI[1,*], H. J. TANG[2,*]

[1]*Institute of Carbon Neutral New Energy Research, Yuzhang Normal University, Nanchang 330031, P. R. China*

[2]*Key Laboratory of Green-Chemistry Materials in University of Yunnan Province, National and Local Joint Engineering Research Center for Green Preparation Technology of Biobased Materials, School of Chemistry & Environment, Yunnan Minzu University, Kuming 650500, PR China*

A novel orange-light-emitting cationic iridium(III) complex $[(ppy)_2Ir(CPO)]PF_6$ (ppy: 2-phenylpyridine, CPO: 2-(4-(3,6-di-tert-butyl-9*H*-carbazol-9-yl)phenyl)-5-(pyridin-2-yl)-1,3,4-oxadiazole) containing a bipolar carbazole-oxadiazole unit was synthesized. Its thermal decomposition temperature (T_d) was 320 °C, and at 100 °C, its photoluminescence (PL) emission intensity was 73.6 % of that at 20 °C. Under the excitation of the GaN-based blue light chips ($\lambda_{em,\ max}$ = 455 nm), the complex was successfully used as phosphors and a red-light component provider in $Y_3Al_5O_{12}:Ce^{3+}$-based white LEDs for converting cold white light into high-quality neutral and warm white light.

(Received December 17, 2023; accepted July 30, 2024)

Keywords: Cationic iridium(III) complex, White light-emitting diode, Photoluminescence, LED, Phosphor

1. Introduction

Relative to traditional light sources (such as incandescent lamps and fluorescent lamps), light-emitting diodes (LEDs) are new artificial light sources with the advantages of high brightness and efficiency, low energy consumption, long life, small size, and environmental protection etc., therefore, they are being widely used and commercialized now [1-9]. Among all kinds of LEDs, white LEDs (WLEDs) are the most important, valuable, and widely used kind. Their wide range of applications includes general illumination, displays, backlighting of liquid crystal display (LCD), automotive headlamps, and so on [1-9]. At present, most WLEDs mainly consisted of blue/ultraviolet chips and phosphors (usually being down-conversion luminescent materials) [1-9]. Especially, the currently commercialized WLEDs are predominantly fabricated by the combination of GaN-based blue light chips and yellow phosphor $Y_3Al_5O_{12}:Ce^{3+}$ ($YAG:Ce^{3+}$), mainly due to the advantages of high efficiency and long life [1-9].

However, because the emission of YAG: Ce^{3+} is mainly located in the yellow light region and lacks a red-light component, so, $Y_3Al_5O_{12}:Ce^{3+}$-GaN-based WLEDs usually emit cold white light with high correlated color temperature (CCT) and low color rendering index (CRI) [10-14]. However, relative to cold white light, neutral and warm white light is softer and it makes people feel more pleasant, comfortable, and peaceful, which is more suitable in some places, such as

bedrooms, hospitals, shopping malls, restaurants, waiting halls, etc. When $Y_3Al_5O_{12}:Ce^{3+}$-GaN-based WLEDs would be converted into neutral and warm WLEDs, their drawbacks must be overcome via red-light component being added. Two methods are usually used to achieve this goal.

i) To modify YAG:Ce^{3+} by some metal ions (such as Pr^{3+} [12], Eu^{3+} [13, 14], Cu^{+} [14], etc.) via doping, which can add some red-emitting on top of yellow light of YAG:Ce^{3+}. However, the metal ions being available for such method are very limited, moreover, the yellow-light-emitting of YAG: Ce^{3+} itself is severely weakened, which results in low luminescent efficiency. Therefore, such method is rarely used in practice.

ii) Adding some red-emitting materials in WLEDs as phosphors. This is a better method because many red-emitting materials (including inorganic and organic luminescent materials) are available for choice.

Nevertheless, due to some unendurable drawbacks, many red phosphors cannot be used for obtaining neutral and warm WLEDs. For example, some red phosphors (such as $K_2SiF_6:Mn^{4+}$, $M_2SiO_4:Eu^{2+}$, M = Ba^{2+}, Sr^{2+}, and Ca^{2+}) are potentially degradable under high temperature and humidity conditions [5]. Some of them show high thermal quenching. For example, the relative emission peak intensity of $Sr_2CeO_4:Eu^{3+}$ at 100 ℃ was less 30% of that at room temperature [15]. Some red phosphors emit deep red light and even near-IR light (such as $Ca_{14}Al_{10}Zn_6O_{35}:Mn^{4+}$ [16]), which is low sensitivity to human eyes. So, it is still very significant to develop and explore new luminescent materials which can emit red-light components (including red, reddish-orange, orange, and even yellowish-orange light) for fabricating neutral and warm $Y_3Al_5O_{12}:Ce^{3+}$-GaN-based WLEDs.

Cationic iridium(III) complexes have been researched and developed for over twenty years, because they are important and promising phosphorescent materials with some significant advantages including high quantum efficiency (up to 100% theoretically), high light-emitting color adjustability via various organic ligands, high stability, short triplet state lifetimes, being easily synthesized and so on [17-25]. They have been widely used in organic light-emitting diodes (OLEDs) [17, 19], light-emitting electrochemical cells (LECs) [17, 18], phosphors in LEDs [20-22], chemiluminescent detection [23], bioimaging [24], photodynamic therapy [25] and so on. In field of phosphors for LEDs, they also are promising candidates [20-22]. In the field of organic luminescent materials (including organic iridium(III) complexes), numerous experimental and theoretical studies have demonstrated that organic bipolar units consisting of electron-donating (such as carbazole, triphenylamine) and electron-absorbing (such as oxadiazole, triazine) functional groups are beneficial in improving luminescent efficiency and brightness, mainly due to charge carrier mobilities being enhanced by the electron push-pull effect of the bipolar units [26-28].

Based on above views, here, a new orange-light-emitting cationic iridium(III) complex containing a carbazole-oxadiazole bipolar unit was designed and synthesized. After its optical and thermal properties are studied, this complex was successfully used as a red-light component provider in $Y_3Al_5O_{12}:Ce^{3+}$-GaN-based WLEDs for converting the cold white light into high-quality neutral and warm white light.

2. Experimental

2.1. Reagents and instruments

All chemicals, reagents, and materials were purchased from Shanghai Titan Technology Co. Ltd (Shanghai, China), and used without further purification.

A Bruker AV400 spectrometer was used for obtaining ^1H NMR spectra, tetramethylsilane (TMS) was used as the internal standard. A Bruker amaZon SL Liquid Chromatography-Mass Spectrometry (LC-MS) with an electrospray ionization (ESI) source was used for measuring mass spectra (MS), acetonitrile was used as solvent. Ultraviolet-visible (UV-vis) absorption spectrum of the cationic iridium(III) complex was measured on an Agilent 8453 UV-visible Spectroscopy System. A Hitachi F-7000 fluorescence spectrophotometer was used for measuring photoluminescence (PL) spectra. In the PL thermal quenching investigation, the temperature of the cationic iridium(III) complex sample was controlled by a temperature controller (REX-C110, Kaituo Compressor

Parts Co. Ltd, Dongguan City, China). Thermogravimetry (TG) was measured on a Netzsch STA449F3 thermal analyzer at a heating rate of 10 °C ·min^{-1} under N_2.

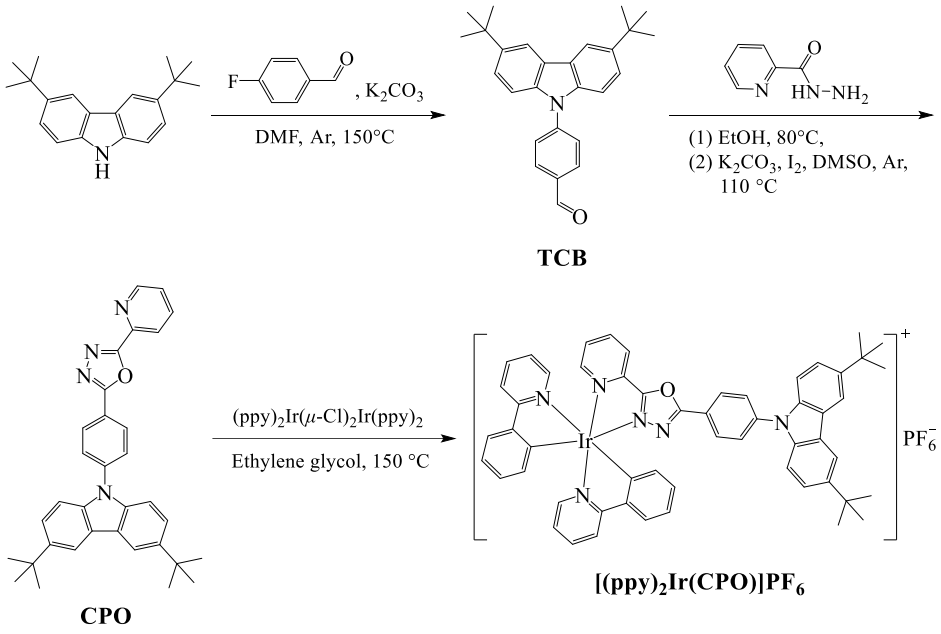

Scheme 1. Synthetic route to [(ppy)$_2$Ir(CPO)]PF$_6$

2.2. Synthesis and characterization of the cationic iridium(III) complex [(ppy)$_2$Ir(CPO)]PF$_6$

The synthetic route to [(ppy)$_2$Ir(CPO)]PF$_6$ is shown in Scheme 1.

2.2.1. Synthesis of 4-(3,6-di-tert-butyl-9H-carbazol-9-yl) benzaldehyde (TCB)

3,6-Di-*tert*-butyl-9*H*-carbazole (5.00 g, 17.9 mmol) was dissolved in dry N, N-dimethylformamide (DMF, 30 mL), a solution of *p*-fluorobenzaldehyde (2.23 g, 18.0 mmol) in DMF was added dropwise into with stirring, then anhydrous K_2CO_3 (7.42 g, 5.38 mmol) was added. The mixture was reacted at 150 °C for 8 h under Ar. The cooled reaction mixture was poured into water (250 mL), stirred for a few moments, and extracted with CH_2Cl_2 (3×50 mL). The organic phase was collected and washed with saturated saline (3×75 mL). After being dried with anhydrous $MgSO_4$ for 8 h, the solvent was removed by a rotary evaporator. The residue was purified by column chromatography on silica gel, using CH_2Cl_2 and petroleum ether (volume rate, 1:1) as eluants. White solid was obtained, yielding 80.7% (5.54 g). ^{1}H NMR (400 MHz, $CDCl_3$, ppm), δ: 10.10 (s, 1H, −CHO), 8.15 (d, 2H, ^3J = 1.2 Hz, ArH), 8.11 (d, 2H, ^3J = 8.4 Hz, ArH), 7.79 (d, 2H, ^3J = 8.4 Hz, ArH), 7.48 (m, 4H, ArH), 1.48 (s, 18H, −CH_3).

2.2.2. Synthesis of 2-(4-(3,6-di-tert-butyl-9H-carbazol-9-yl) phenyl)-5-(pyridin-2-yl)-1,3,4-oxadiazole (CPO)

Picolinohydrazide was synthesized according to the reported procedure [29]. TCB (2.83 g, 10.0 mmol) and picolinohydrazide (1.51 g, 11.0 mmol) were dissolved in ethanol (20 mL) and refluxed for 8 h under Ar, then the solvent was removed by a vacuum rotary evaporator. The resultant light-green powders were dissolved in dimethyl sulfoxide (DMSO, 20 mL), anhydrous K_2CO_3 (4.14 g, 30.0 mmol), and I_2 (3.81 g, 15.0 mmol) were added, the reaction mixture was refluxed with stirring under Ar for 4 h. After being cooled to room temperature, a solution of $Na_2S_2O_3$ (5.0%) was added dropwise in until the

brownish black disappeared. The mixture was poured into water (250 mL) and extracted with CH_2Cl_2 (3 × 50 mL). The organic phase was collected and washed with saturated saline (3×75 mL). After being dried with anhydrous $MgSO_4$ for 8 h, the solvent was removed by a rotary evaporator. The residue was purified by silica gel column chromatography, using CH_2Cl_2 and petroleum ether (volume rate, 1:1) as eluants. White solid was obtained, yielding 76.4% (3.82 g). ^{1}H NMR (400 MHz, $CDCl_3$, ppm), δ: 8.85 (d, 1H, ^3J = 4.8 Hz, ArH), 8.45 (d, 2H, ^3J = 4.8 Hz, ArH), 8.37 (d, 1H, ^3J = 8.0 Hz, ArH), 8.15 (s, 2H, ArH), 7.94 (t, 1H, ^3J = 7.8 Hz, ArH), 7.78 (d, 2H, ^3J = 8.4 Hz, ArH), 7.44−7.53 (m, 5H, ArH), 1.48 (s, 18H, $-CH_3$).

2.2.3. Synthesis of [(ppy)$_2$Ir(CPO)]PF$_6$

The dimer $(ppy)_2Ir(\mu\text{-}Cl)_2Ir(ppy)_2$ (ppy: 2-phenylpyridine) was synthesized according to the literature [30]. The dimer (0.69 g, 0.65 mmol) and CPO (0.65 g, 1.3 mmol) were added into ethylene glycol (25 mL) and heated to 60 °C with stirring under Ar for 30 min, then the temperature was raised to 150 °C and kept for 16 h. After the reaction mixture being cooled, a solution of NH_4PF_6 in water (1.0 mol·L^{-1}, 10 mL) was added. Then, the resulting yellow suspension was filtered, washed with water, dried at 80 °C for 10 h, and purified by silica gel column chromatography, using CH_2Cl_2 and CH_3CN (volume rate, 5:1) as eluants. Orange-yellow solid was obtained, yield 52.6% (0.79 g). ^{1}H NMR (400 MHz, $CDCl_3$, ppm), δ: 8.74 (d, 1H, ^3J = 8.0 Hz, ArH), 8.31−8.44 (m, 6H, ArH), 8.26 (d, 2H, ^3J = 8.4 Hz, ArH), 7.86−8.00 (m, 8H, ArH), 7.70 (d, 1H, ^3J = 5.6 Hz, ArH), 7.52 (d, 2H, ^3J = 8.8 Hz, ArH), 7.41 (d, 2H, ^3J = 8.8 Hz, ArH), 7.23 (t, 2H, ^3J = 7.8 Hz, ArH), 7.04 (t, 1H, ^3J = 8.0 Hz, ArH), 6.90−6.98 (m, 2H, ArH), 6.84 (td, 1H, ^3J = 8.0 Hz, ^4J = 1.0 Hz, ArH), 6.15 (dd, 2H, ^3J = 7.6 Hz, ^4J = 2.8 Hz, ArH), 1.41 (s, 18H, $-CH_3$). MS (*m*/*z*, ESI$^+$): calc. for $C_{55}H_{48}F_6IrN_6OP$, 1001.35 $[M-PF_6]^+$; found, 1001.50 $[M-PF_6]^+$.

2.3. Preparation and performance measurements of LEDs

In this work, the LEDs using the complex $[(ppy)_2Ir(CPO)]PF_6$ or/and $Y_3Al_5O_{12}$:Ce^{3+} as phosphors and GaN-based blue light chips ($\lambda_{em,\ max}$ = 455 nm) as excitation light sources were fabricated. The phosphors were blended in silicone resin at different concentrations (listed in Table 1), stirred homogeneously, and then coated on the surface of the chips until the reflective cavities were filled up. The LEDs were slowly heated to 80 °C and kept for 30 min, then were solidified at 150 °C for 1 h. Emission spectra and light-emitting performances of all LEDs were recorded on a highly accurate array spectrometer (HSP6000) and an integrating sphere spectroradiometer system (PMS-50), respectively, Everfine Optoelectronics Technology Co. Ltd, Hangzhou, China.

Table 1. Performance data of the LEDs

No. of LEDs	Blending concentrations (wt%)		LE (lm·W^{-1})	CRI	CCT (K)	$\lambda_{em.max}$ (nm)	CIE (x,y)
	YAG:Ce^{3+}	complex					
1	7.0	0.0	142.85	73.5	6593	457, 549	(0.31, 0.33)
2	7.0	0.5	91.4	81.2	5218	458, 578	(0.34, 0.31)
3	7.0	1.0	88.5	78.7	4115	459, 578	(0.36, 0.34)
4	7.0	2.0	62.7	74.0	3480	458, 579	(0.40, 0.37)
5	0	4.0	10.3	55.5	1788	604	(0.56, 0.41)

3. Results and discussion

3.1. UV-vis absorption property

The UV-vis absorption (Abs) spectrum of the complex $[(ppy)_2Ir(CPO)]PF_6$ in CH_2Cl_2 (1.0×10^{-5}mol·L^{-1}) is shown in Fig. 1. The absorption spectrum of the complex consisted of two parts. The first part was mainly located at 200~365 nm containing three peaks with the maximum absorption wavelengths ($\lambda_{abs,max}$) of 242 nm, 290 nm, and 338 nm, their molar extinction coefficients (ε) were 1.46×10^5 L·mol^{-1}·cm^{-1}, 9.80×10^4 L·mol^{-1}·cm^{-1}, and 3.88×10^4 L·mol^{-1}·cm^{-1}, respectively. The absorption of this part was mainly caused by the spin-allowed singlet π-π* (^{1}π-π*) ligand-centered (LC) transition [19, 20, 23, 28]. The second part mainly located at 365~500 nm with the $\lambda_{abs,\ max}$ of 403 nm (ε = 3.43×10^4 L·mol^{-1}·cm^{-1}), this part mainly was the overlapping absorption caused by singlet and triplet metal–to–ligand charge transfer (^{1}MLCT and ^{3}MLCT), singlet and triplet ligand–to–ligand charge transfer (^{1}LLCT and ^{3}LLCT) and ^{3}π–π* LC transition [19, 20, 23, 28]. This absorption part usually is very weak for many iridium(III) complexes [19, 23, 31], however, $[(ppy)_2Ir(CPO)]PF_6$ showed strong absorption at this part, mainly due to high intramolecular charge transfer caused by the carbazole-oxadiazole bipolar unit [20, 28]. As shown in Fig. 1, the absorption spectrum of the complex observably overlapped with the electroluminescence (EL) spectrum of GaN-based blue light chip, which suggested the complex can be excited by the blue light of the chips. However, the absorption spectrum hardly overlapped with the photoluminescence (PL) spectrum of YAG: Ce^{3+}, which implied the light-emitting of YAG:Ce^{3+} would hardly be affected by the complex when they were used together.

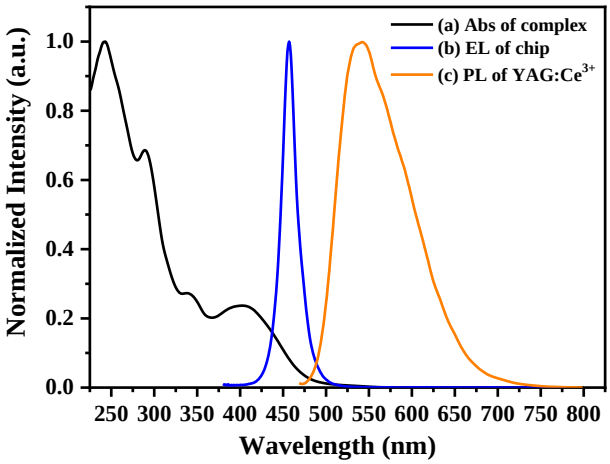

Fig. 1. (a) UV-vis Abs spectrum of $[(ppy)_2Ir(CPO)]PF_6$ in CH_2Cl_2 at 1.0×10^{-5}mol·L^{-1}; (b) EL spectrum of a GaN-based blue light chip ($\lambda_{em.max}$ = 455 nm); (c) PL spectrum of YAG:Ce^{3+} (color online)

3.2. PL property

PL excitation (Ex) and emission (Em) spectra of $[(ppy)_2Ir(CPO)]PF_6$ in CH_2Cl_2 (1.0×10^{-5} mol·L^{-1}), in silicone resin (at 4.0 wt.%) and in solid powders state were measured at room temperature and the results are shown in Fig. 2. The maximum emission wavelengths ($\lambda_{em,\ max}$) of emission spectra of the complex in above-mentioned three states were 624 nm, 604 nm, and 582 nm, three spectra corresponded to red, orange, and yellowish orange, respectively. They were blue shift sequentially, which was probably caused by the dendritic tert-butyls on carbazole, because the coplanarity of the carbazole, benzene, oxadiazole, and pyridine in the ancillary ligand CPO would be affected by the tert-butyls and decrease with increasing aggregation of the complex. Lower coplanarity meant lower π-electron conjugated system and wider energy gap, which further meant light-emitting would be in shorter wavelength range. Such coplanarity would not be greatly affected when the complex was in solution at a very low concentration, relatively, the complex being blended in silicone resin at a low concentration (at 4.0 wt%) was in the middle situation, the complex in solid powders had the highest degree of aggregation. Moreover, the sequential blue shift also may be caused by weaker vibrational coupling between the emitting state T_1 and the ground state S_0 in

higher aggregation state and the resulting bigger separation between them [22].

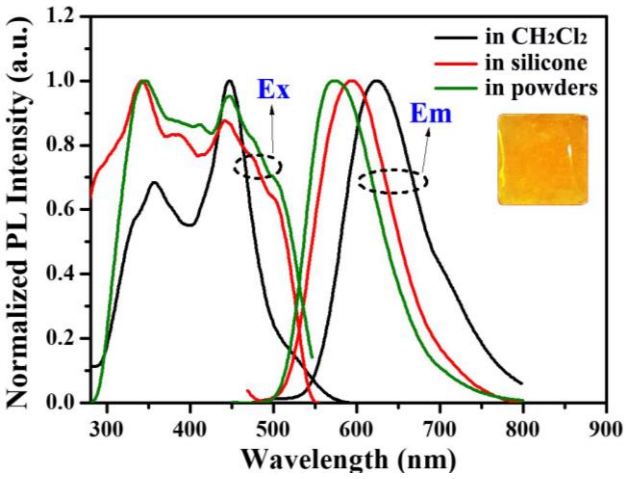

Fig. 2 PL excitation (Ex) and emission (Em) spectra of $[(ppy)_2Ir(CPO)]PF_6$ in CH_2Cl_2 (1.0×10^{-5} mol·L^{-1}, λ_{ex} = 445 nm, λ_{em} = 625 nm), in silicone resin (at 4.0 wt.% , λ_{ex} = 445 nm, λ_{em} = 604 nm) and in pure powders state (λ_{ex} = 447 nm, λ_{em} = 582 nm). Insert photograph: the light-emitting state of $[(ppy)_2Ir(CPO)]PF_6$ in silicone resin (at 4.0 wt.%) under 450 nm blue light (color online)

The excitation spectra of the complex in three situations all were mainly located at 300~550 nm, and all overlapped with the whole EL spectra of the blue light chips ($\lambda_{em,\,max} \approx 455$ nm, Fig. 1), which also suggested that $[(ppy)_2Ir(CPO)]PF_6$ can be efficiently excited by the chips and it was a suitable phosphor for above-mentioned $Y_3Al_5O_{12}:Ce^{3+}$-based WLEDs.

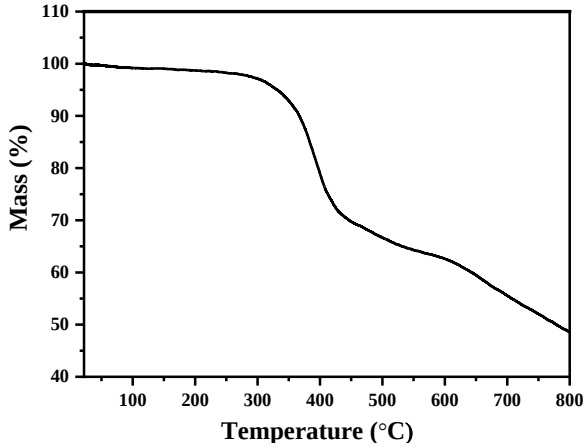

Fig. 3. TG curve of $[(ppy)_2Ir(CPO)]PF_6$, 10 °C/min, under N_2

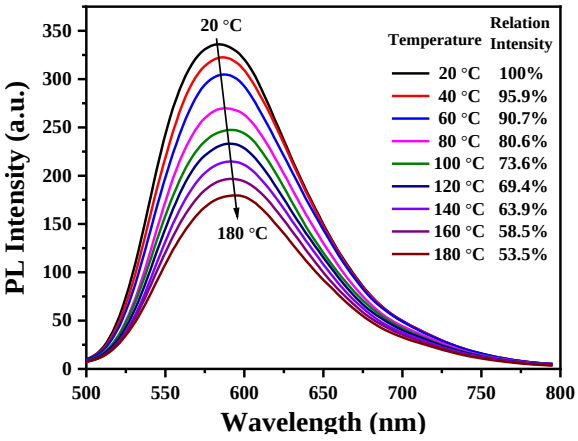

Fig. 4. Temperature-dependent PL spectra (from 20 °C to 180 °C, λ_{ex} = 455 nm) of $[(ppy)_2Ir(CPO)]PF_6$ powders (color online)

3.3. Thermal stability and thermal quenching property

During the preparation of LEDs, LEDs need to undergo heat treatment, moreover, the working process of LEDs is an inevitable exothermic process, so, thermal stability and thermal quenching properties of phosphors need to be investigated. The TG curve of $[(ppy)_2Ir(CPO)]PF_6$ powders was measured, the result is shown in Fig. 3. From room temperature to 150 ℃, there was a very tiny mass loss of about 0.97%, which was mainly caused by the volatilization of adsorptive water and residual organic solvents. Then, the curve became very flat, which meant there was almost no loss of mass. However, after 320 °C, significant and quick mass loss began to occur, which suggested the complex began to undergo thermal decomposition and 320 °C was its thermal decomposition temperature (T_d). Because the required heat-resistant temperature for phosphors being used in LEDs is usually below 150 ℃ [20, 22], so this T_d is high enough.

The complex powders sample was heated from 20 °C to 180 °C for studying its thermal quenching property. The PL spectra (λ_{ex} = 455 nm) were measured every 20 °C and shown in Fig. 4. From 20 °C to 180 °C, the $\lambda_{em,max}$ changed from 583 nm to 593 nm and showed a small red shift of 10 nm. However, the range and shape of all PL spectra had hardly changed, which suggested the light-emitting color was basically stable and

unchanged with the increasing temperature. The emission intensity gradually declined with the increasing temperature (i.e., thermal quenching), relative to the PL emission intensity (as 100.0 %) at initial 20 °C, the intensities at other temperatures are 95.9 % (at 40 °C), 90.7 %(at 60 °C), 80.6 % (at 80 °C), 73.6 % (at 100 °C), 69.4 % (at 120 °C), 63.9 % (at 140 °C), 58.5 % (at 160 °C), and 53.5 % (at 180 °C), respectively. Compared with the thermal quenching of other luminescent materials in the literatures [15, 16, 20, 22], the thermal quenching of $[(ppy)_2Ir(CPO)]PF_6$ was in the middle level, and $[(ppy)_2Ir(CPO)]PF_6$ was applicable for LEDs.

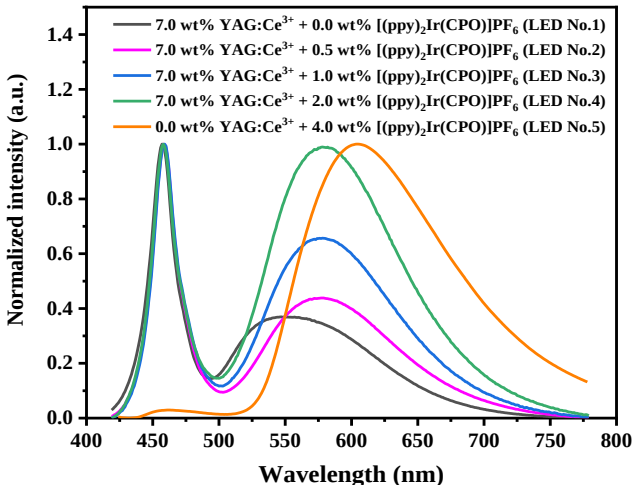

Fig. 5. Luminescence spectra of LEDs No.1-5 (color online)

3.4. Application in LEDs

Five LEDs were fabricated, as listed in Table 1. As for LED No.1, only 7.0 wt% $YAG:Ce^{3+}$ was used as phosphors without any $[(ppy)_2Ir(CPO)]PF_6$. This LED was a typical commercial WLED which consisted of yellow-emitting $YAG:Ce^{3+}$ (7.0 wt% in silicane resin) and a GaN-based blue light chip ($\lambda_{em,max} \approx 455$ nm). Its CCT was 6593 K, its CRI was 73.5, which suggested it was a WLED emitting cold white light with relatively low CRI. Together with $YAG:Ce^{3+}$ (still at 7.0 wt%), when $[(ppy)_2Ir(CPO)]PF_6$ was added as phosphors at 0.5 wt% (LED No.2) and 1.0 wt% (LED No.3), two WLEDs emitting neutral white light were obtained, their CCTs were 5218 K and 4115 K, their CRIs were 81.2 and 78.7, respectively. The CCTs of WLEDs had been reduced, while their CRIs had been increased due to the red-light component from the complex being added to their spectra. As shown in Fig. 5, the spectra of LEDs No.1-3 all consisted of two peaks, the left peaks ($\lambda_{em,max} \approx 458$ nm) were the light-emitting of the blue light chips, the right peaks were the light-emitting of $YAG:Ce^{3+}$ (LED No.1) or the light-emitting of $YAG:Ce^{3+}$ together with $[(ppy)_2Ir(CPO)]PF_6$ (LED No.2 and 3). The right peaks of LEDs No.2 and No.3 were wider than that of LED No.1, their $\lambda_{em,max}$ (578 nm) also showed an obvious red shift relative to that of LED No.1 (549 nm). With the increasing usage amounts of the complex, the right peaks became relatively higher and higher, and the blue light of chips became weaker and weaker. LED No.3 became a WLED emitting warm white light. Its CCT was 3480 K, and its CRI was 74.0, respectively. LED No.5 was fabricated by blue light chip and only $[(ppy)_2Ir(CPO)]PF_6$ (without $YAG:Ce^{3+}$) at 4.0 wt%. Its spectrum showed that the complex had almost completely absorbed the blue light of the chip, so its spectrum almost completely was the orange-light-emitting of the complex ($\lambda_{em,max} = 604$ nm).

As shown in Fig. 6, the Commission Internationale de L´Eclairage (CIE) chromaticity coordinates of LEDs No.1−5 showed a similar change as their CCTs and light colors. LEDs No.1−4 all were WLEDs. Their CIE values changed from (0.31, 0.33) of No.1 (cold WLEDs) to (0.34, 0.31) of No.2 (neutral WLEDs) and (0.36, 0.34) of No.3 (neutral WLEDs), and then to (0.40, 0.37) of No. 4 (warm WLEDs). The CIE value of LED No.5 (emitting orange light) was (0.56, 0.41). The working state photographs of LEDs No.1-5 in Fig. 6 visually showed these successive changes. Due to the impossibility of 100% energy conversion, luminous efficacies (LEs) of LEDs No.1−5 successively decreased with the increasing usage amounts of the complex. Nevertheless, the WLEDs all had high LEs, such as the LE of the warm WLED (No.4) still had 62.7 $lm \cdot W^{-1}$, although this is the lowest value of these WLEDs.

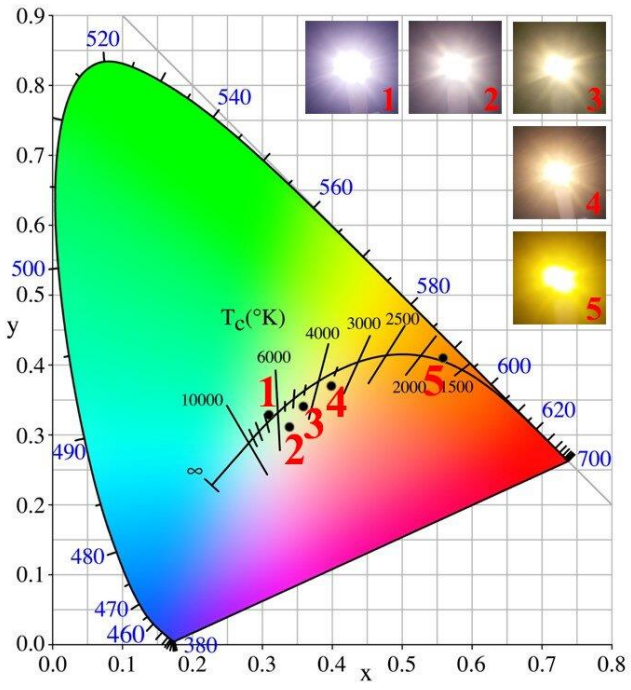

Fig. 6. CIE chromaticity coordinates of LEDs No.1−5. Insert photographs: the working state of LEDs No.1−5 (color online)

4. Conclusion

The $[(ppy)_2Ir(CPO)]PF_6$ containing a carbazole-oxadiazole bipolar unit was successfully synthesized, which can be efficiently excited by blue light chips and emitted bright orange light. Its T_d was as high as 320 °C. At 100 °C, its PL emission intensity was 73.6 % of that at 20 °C. It was successfully used as a phosphor and a red-light component provider in $Y_3Al_5O_{12}:Ce^{3+}$-GaN-based WLEDs for converting cold white light into high-quality neutral and warm white light.

Acknowledgments

This work was supported by Science and Technology Research Project of Education Department of Jiangxi Province (Grant No. GJJ213108), 2021 University-Level Scientific Research Project of Yuzhang Normal University (Grant No. YZYB-21-16), and National Natural Science Foundation of China (No. 21762049 and 21262046).

References

[1] G. B. Nair, H. C. Swart, S. J. Dhoble, Prog. Mater. Sci. **109**, 100622 (2020).

[2] H. Zhang, H. Zhang, A. Pan, B. Yang, L. He, Y. Wu, Adv. Mater. Technol. **6**(1), 2000648 (2020).

[3] J. Cho, J. H. Park, J. K. Kim, E. F. Schubert, Laser Photonics Rev. **11**(2), 1600147 (2017).

[4] J. Y. Tsao, M. H. Crawford, M. E. Coltrin, A. J. Fischer, D. D. Koleske, G. S. Subramania, G. T. Wang, J. J. Wierer, R. F. Karlicek, Adv. Opt. Mater. **2**(9), 809 (2014).

[5] A. A. Setlur, R. J. Lyons, J. E. Murphy, N. Prasanth Kumar, M. Satya Kishore, ECS J. Solid State Sci. Technol. **2**(2), R3059 (2013).

[6] M. F. Prodanov, S. K. Gupta, C. Kang, M. Y. Diakov, V. V. Vashchenko, A. K. Srivastava, Small **17**(3), 2004487 (2020).

[7] Q. Mo, C. Chen, W. Cai, S. Zhao, D. Yan, Z. Zang, Laser Photonics Rev. **15**(10), 2100278 (2021).

[8] H. Tang, Q. Chen, S. Lu, X. Li, H. Li, Y. Wang, K. Wang, Q. Zhou, Z. Wang, J. Lumin. **244**, 118734 (2022).

[9] L. Chen, C.-C. Lin, C.-W. Yeh, R.-S. Liu, Materials **3**(3), 2172 (2010).

[10] H. S. Jang, Y. H. Won, D. Y. Jeon, Appl. Phys. B **95**(4), 715 (2009).

[11] H. H. Kwak, S. J. Kim, Y. S. Park, H. H. Yoon, S. J. Park, H. W. Choi, Mol. Cryst. Liq. Cryst. **513**(1), 106 (2009).

[12] H. S. Jang, W. B. Im, D. C. Lee, D. Y. Jeon, S. S. Kim, J. Lumin. **126**(2), 371 (2007).

[13] Y. Yang, J. Li, B. Liu, Y. Zhang, X. Lv, L. Wei, X. Wang, J. Xu, H. Yu, Y. Hu, H. Zhang, L. Ma, J. Wang, Chem. Phys. Lett. **685**, 89 (2017).

[14] C. Zhao, D. Zhu, M. Ma, T. Han, M. Tu, J. Alloys Compd. **523**, 151 (2012).

[15] H. Li, R. Zhao, Y. Jia, W. Sun, J. Fu, L. Jiang, S. Zhang, R. Pang, C. Li, ACS Appl. Mater. Inter. **6**(5), 3163 (2014).

[16] W. Lü, W. Lv, Q. Zhao, M. Jiao, B. Shao, H. You, Inorg. Chem. **53**(22), 11985 (2014).

[17] D. Ma, T. Tsuboi, Y. Qiu, L. Duan, Adv. Mater. **29**(3), 1603253 (2016).

[18] C. E. Housecroft, E. C. Constable, Chem. Soc. Rev. **350**, 155 (2017).

[19] M. Tian, R. Yu, M. Chen, L. He, Dyes Pigments **193**, 109477 (2021).

[20] H. Tang, Y. Ye, Q. Chen, M. Ren, X. Li, H. Li, Y. Wang, K. Wang, Q. Zhou, Z. Wang, Opt. Mater. **110**, 110382 (2020).

[21] C. Ezquerro, E. Fresta, E. Serrano, E. Lalinde, J. García-Martínez, J. R. Berenguer, R. D. Costa, Mater. Horiz. **6**(1), 130 (2019).

[22] H. Li, Y. Wang, K. Yang, H. Tang, X. Li, G. Meng, S. Lu, L. Gao, K. Wang, Q. Zhou, Z. Wang, Opt. Mater. **124**, 112020 (2022).

[23] H. Tang, Y. Wang, Z. Chen, K. Yang, J. Qin, X. Li, H. Li, L. Gao, S. Lu, K. Wang, Spectrochim. Acta A Mol. Biomol. Spectrosc. **279**, 121396 (2022).

[24] Q. Zhao, C. Huang, F. Li, Chem. Soc. Rev. **40**(5), 2508 (2011).

[25] A. Zamora, G. Vigueras, V. Rodríguez, M. D. Santana, J. Ruiz, Coord. Chem. Rev. **360**, 34 (2018).

[26] O. Ostroverkhova, Chem Rev. **116**(22), 13279 (2016).

[27] W.-Y. Wong, C.-L. Ho, Coord. Chem. Rev. **253**(13-14), 1709 (2009).

[28] H. Tang, Y. Li, Q. Chen, B. Chen, Q. Qiao, W. Yang, H. Wu, Y. Cao, Dyes Pigments **100**, 79 (2014).

[29] X. Zhao, X.-Z. Wang, X.-K. Jiang, Y.-Q. Chen, Z.-T. Li, G.-J. Chen, J. Am. Chem. Soc. **125**, 15128 (2003).

[30] T. Peng, G. Li, K. Ye, C. Wang, S. Zhao, Y. Liu, Z. Hou, Y. Wang, J. Mater. Chem. C **1**(16), 2920 (2013).

[31] L.-P. Li, B. H. Ye, Inorg. Chem. **58**(12), 7775 (2019).

*Corresponding author: wyq_kikiemail@163.com
tanghuaijun@sohu.com